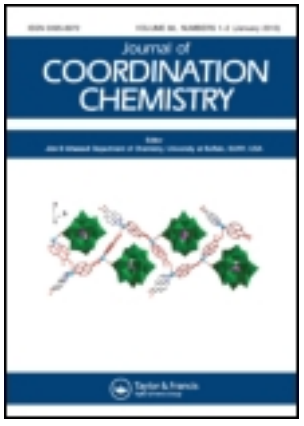

Journal of Coordination Chemistry
Publication details, including instructions for authors and subscription information:
http://www.tandfonline.com/loi/gcoo20

Synthesis, crystal structure, and properties of three supramolecular compounds based on Keggin-type phosphomolybdate and different flexible ligands

Mingli Qi[ab], Kai Yu[ab], Zhanhua Su[ab], Chunxiao Wang[ab], Chunmei Wang[ab], Baibin Zhou[ab] & Chuncheng Zhu[ab]

[a] Key Laboratory for Photonic and Electronic Bandgap Materials, Ministry of Education, Harbin Normal University, Harbin, P.R. China

[b] Key Laboratory of Synthesis of Functional Materials and Green Catalysis, College of Heilongjiang Province, Harbin Normal University, Harbin, P.R. China

Accepted author version posted online: 16 Sep 2013.Published online: 06 Nov 2013.

To cite this article: Mingli Qi, Kai Yu, Zhanhua Su, Chunxiao Wang, Chunmei Wang, Baibin Zhou & Chuncheng Zhu (2013) Synthesis, crystal structure, and properties of three supramolecular compounds based on Keggin-type phosphomolybdate and different flexible ligands, Journal of Coordination Chemistry, 66:20, 3531-3543, DOI: 10.1080/00958972.2013.844801

To link to this article: http://dx.doi.org/10.1080/00958972.2013.844801

Journal of Coordination Chemistry, 2013
Vol. 66, No. 20, 3531–3543, http://dx.doi.org/10.1080/00958972.2013.844801

Synthesis, crystal structure, and properties of three supramolecular compounds based on Keggin-type phosphomolybdate and different flexible ligands

MINGLI QI†‡,, KAI YU†‡,, ZHANHUA SU†‡,, CHUNXIAO WANG†‡,, CHUNMEI WANG†‡,, BAIBIN ZHOU*†‡ and CHUNCHENG ZHU†‡

†Key Laboratory for Photonic and Electronic Bandgap Materials, Ministry of Education, Harbin Normal University, Harbin, P.R. China
‡Key Laboratory of Synthesis of Functional Materials and Green Catalysis, College of Heilongjiang Province, Harbin Normal University, Harbin, P.R. China

(*Received 5 July 2013; accepted 21 August 2013*)

Three supramolecular compounds based on Keggin phosphomolybdate and different flexible ligands, $Cu_3(bei)_6(PMo_{12}O_{40})_2 \cdot 6H_2O$ (**1**), $(H_2bbi)(Hbbi)(PMo_{12}O_{40}) \cdot 2H_2O$ (**2**), and $(H_2bpp)_3(PMo_{12}O_{40})_2 \cdot 6H_2O$ (**3**) (bei = 1,1′-(1,2-ethanediyl)bis(imidazole), bbi = 1,1′-(1,4-butanediyl)bis(imidazole), bpp = 1,3-bi (4-pyridyl)propane)), have been hydrothermally prepared and characterized by elemental analysis, IR, TG, XRD, and single-crystal XRD. Crystal data analysis reveals that **1**–**3** are composed of discrete $[Cu(bei)_2]^{2+}$ complex cations, protonated bbi and bpp cations, respectively, with $[PMo_{12}O_{40}]^{3-}$. All three compounds exhibit interesting supramolecular frameworks via electrostatic interactions and hydrogen bonds. Their electrochemistry, electrocatalytic behavior, and solid state fluorescence at room temperature have been investigated.

Keywords: Supramolecular; $PMo_{12}O_{40}^{3-}$; Flexible ligand; Electrochemical character; Fluorescent property

1. Introduction

Design and synthesis of organic–inorganic supramolecular compounds have received attention for structural diversity and versatile physical and chemical properties, such as catalysis, sorption, magnetism, electrical conductivity, biological activities, nonlinear optical materials, molecular recognition, and photosensitive materials [1–11]. Organic–inorganic supramolecular compounds have widespread interest [12, 13]. However, compounds composed of polyoxometalates (POM) and flexible ligands are scarce. Therefore, it is necessary to enrich this branch, which may obtain more POM-based supramolecular compounds.

POMs, as a large family of metal–oxygen clusters, are outstanding inorganic building blocks due to their structures, controllable sizes, shapes, and high negative charges [14–21]. In this subfamily, the Keggin species $[XM_{12}O_{40}]^{n-}$ (X = B, P, Si, etc.; M = Mo and W),

*Corresponding author. Email: zhou_bai_bin@163.com

especially, $[PMo_{12}O_{40}]^{3-}$ POMs remain comparatively less to be employed as candidates to incorporate transition metals and organic ligands into multidimensional topological architectures, probably because of their unstable structure, and only a few compounds have been reported [22–25].

Flexible ligands, in particular, alkyl-based bis(imidazole) or bis(pyridine) ligands with flexible skeletons, the $–(CH_2)_n–$ spacers, allow themselves to bend and rotate freely so as to conform to the coordination geometries of POM anions to yield fascinating structures in the assembly process [26–28]. However, more attention has been paid to assembly of $[PMo_{12}O_{40}]^{3-}$ POM complexes with rigid cations [29–33]. Compounds composed of alkyl-based bis(imidazole) or bis(pyridine) flexible ligands are still very rare [34–36], and most are metal–organic coordination polymers [37–39]. Both $[PMo_{12}O_{40}]^{3-}$ and alkyl-based bis(imidazole) or bis(pyridine) flexible ligand cations coexist in only one supramolecular compound.

Herein, based on our previous work [40–42], we chose the classical Keggin-type POM ($[PMo_{12}O_{40}]^{3-}$) as inorganic building block and three flexible ligands, bei, bbi, and bpp. Three new PMo_{12}-based supramolecular compounds, $Cu_3(bei)_6(PMo_{12}O_{40})_2·6H_2O$ (**1**), $(H_2bbi)(Hbpi)(PMo_{12}O_{40})·2H_2O$ (**2**), and $(H_2bpp)_3(PMo_{12}O_{40})_2·6H_2O$ (**3**), have been prepared and characterized. Their electrochemistry, electrocatalytic behaviors, and solid state fluorescence at room temperature have been studied; all the title compounds have good electrocatalytic activity and are potential fluorescent materials.

2. Experimental

2.1. *Materials and general procedures*

All reagents were purchased commercially and used without purification. $H_3PMo_{12}O_{40}·13H_2O$ was prepared according to a literature method [43] and verified by the IR spectrum. Elemental analyzes (C, H, and N) were performed on a Perkin–Elmer 2400 CHN Elemental Analyzer. P, Mo, and Cu analyzes were performed on a PLASMA-SPEC (I) inductively coupled plasma atomic emission spectrometer. IR spectra were obtained on an Alpha Centaurt FT/IR spectrometer with KBr pellets from 400 to 4000 cm^{-1}. Thermal gravimetric analyzes (TGA) were carried out in N_2 on a Perkin–Elmer DTA 1700 differential thermal analyzer with a rate of 10 °C/min. XRD patterns were collected on a Rigaku Dmax 2000 X-ray diffractometer with graphite-monochromated Cu Kα radiation (λ = 0.154 nm) and 2θ ranging from 5° to 50°. Fluorescence spectra were performed on a Hitachi F-4500 fluorescence/phosphorescence spectrophotometer with a 450 W xenon lamp as the excitation source. Electrochemical measurements were taken with a CHI660 electrochemical workstation. A conventional three-electrode system was used. The working electrode was a carbon paste electrode (CPE), a Pt wire was the counter electrode, and Ag/AgCl (3 M KCl) electrode was used as a reference electrode.

2.2. *Synthesis of 1*

A mixture of $H_3PMo_{12}O_{40}·13H_2O$ (0.6187 g, 0.3 mM), $(CH_3COO)_2Cu·H_2O$ (0.16 g, 0.8 mM), bei (0.0324 g, 0.2 mM), and H_2O (16 mL) was stirred for 30 min in air until it was homogeneous. When the pH of the mixture was adjusted to 4–5 with 1 M HCl, the

solution was transferred and sealed in a 30-mL Teflon-lined stainless steel autoclave, which was heated at 160 °C under autogenous pressure for 3 days. The dark green block crystals were isolated and collected by filtration, washed thoroughly with distilled water, and dried at room temperature (56% yield based on Mo). Anal. $C_{48}H_{72}Cu_3Mo_{24}N_{24}O_{86}P_2$ (4927.87): C, 11.89 (Calcd 11.86); H, 1.34 (1.46); N, 6.89 (6.92); P, 1.31 (1.28); Mo, 47.49(47.45); Cu, 3.83(3.90) wt.%.

2.3. *Synthesis of 2*

A mixture of $H_3PMo_{12}O_{40}{\cdot}13H_2O$ (0.4125 g, 0.2 mM), bbi (0.0760 g, 0.4 mM), and H_2O (16 mL) was stirred for 30 min in air until it was homogeneous. When the pH of the mixture was adjusted to 4–5 with 1 M HCl, the solution was transferred and sealed in a 30-mL Teflon-lined stainless steel autoclave, which was heated at 170 °C under autogenous pressure for 5 days. The light green block crystals were isolated and collected by filtration, washed thoroughly with distilled water, and dried at room temperature (43% yield based on Mo). Anal. $C_{20}H_{28}Mo_{12}N_8O_{42}P$ (2238.75): C, 10.64 (Calcd 10.72); H, 1.29 (1.43); N, 4.93 (5.00); P, 1.42 (1.38); Mo, 51.57 (51.46) wt.%.

2.4. *Synthesis of 3*

A mixture of $(NH_4)_6Mo_7O_{24}{\cdot}4H_2O$ (0.5 g, 0.4046 mM), bpp (0.10 g, 0.5044 mM) H_2O (10 mL), and C_2H_5OH (5 mL) was stirred for 30 min in air until it was homogeneous. When the pH of the mixture was adjusted to 4–5 with 1 M HCl, the solution was transferred and sealed in a 30-mL Teflon-lined stainless steel autoclave, which was heated at 140 °C under autogenous pressure for 5 days. The dark green block crystals were isolated and collected by filtration, washed thoroughly with distilled water, and dried at room temperature (56% yield based on Mo). Anal. $C_{39}H_{54}P_2Mo_{24}N_6O_{86}$ (4350.38): C, 10.71 (Calcd 10.76); H, 1.29 (1.24); N, 1.88 (1.93); P, 1.42 (1.43); Mo, 52.98 (52.93) wt.%.

2.5. *Preparation of 1-, 2- and 3-CPEs*

Complexes **1**, **2**, and **3** modified CPEs **1**-, **2**- and **3**-CPEs were prepared as follows: 300 mg of graphite powder and 30 mg of complex were mixed and ground together by agate mortar and pestle to achieve a uniform mixture. To the mixture, three drops of Nujol was added with stirring. The homogenized mixture was packed into a glass tube with 3 mm inner diameter, and the surface was pressed tightly onto weighing paper with a copper rod through the back. Electrical contact was established with a copper rod through the back of the electrode.

2.6. *X-ray crystallography*

The crystal structures of the three compounds were determined from single-crystal XRD data. Intensity data were collected on a Bruker SMART CCD diffractometer equipped with graphite-monochromated Mo-Kα radiation (λ = 0.71073 Å). The structure was solved by direct methods and difference Fourier map with SHELXL-97 [44, 45] and refined by full-matrix least-squares on F^2. Anisotropic thermal parameters were used to refine all non-hydrogen atoms. The positions of hydrogens of organic molecules were calculated

Table 1. Crystal data and structure refinement details for **1**–**3**.

	1	**2**	**3**
Empirical formula	$C_{48}H_{72}Mo_{24}N_{24}O_{86}P_2Cu_3$	$C_{20}H_{28}Mo_{12}N_8O_{42}P$	$C_{39}H_{54}Mo_{24}N_6O_{86}P_2$
M	4927.87	2238.75	4350.38
λ/Å	0.71073	0.71073	0.71073
T/K	273(2)	296(2)	273(2)
Crystal dimensions/mm	0.26 × 0.24 × 0.20	0.26 × 0.24 × 0.24	0.26 × 0.24 × 0.20
Crystal system	Trigonal	Triclinic	Trigonal
Space group	*R* –3	*P* –1	*R* –3
Unit cell dimensions	a = 20.4798(4), b = 20.4798(4), c = 24.1147(11), α = 90, β = 90, γ = 120	a = 11.3208(8), b = 11.6816(9), c = 11.8596(9), α = 102.0810(10), β = 98.0630(10), γ = 116.8150(10)	a = 18.3213(6), b = 18.3213(6), c = 25.3251(16), α = 90, β = 90, γ = 120
V/Å^3	8759.2(6)	1318.31(17)	7362.0(8)
Z	3	1	3
D_c/Mg m^{-3}	2.755	2.815	2.942
μ/mm^{-1}	3.157	2.896	3.106
F (0 0 0)	6807	1059	6168
θ range/°	2.45–28.37	2.29–28.26	2.942–28.28
Measured reflections	21,984	10,713	18,595
Independent reflections	4874	6284	7856
Data/restraints/parameters	4874/0/283	6284/12/394	7856/1/472
R_{int}	0.0169	0.0165	0.0176
$R_1(I > 2\sigma(I))$[a]	0.0318	0.0425	0.0201
wR_2 (all data)[a]	0.0818	0.1102	0.0473
Goodness-of-fit on F^2	1.043	1.035	1.001

[a] $R_1 = \sum ||F_0| - |F_C|| / \sum F_0|; wR_2 = \sum [w(F_0^2 - F_C^2)^2] / \sum [w(F_0^2)^2]^{1/2}$.

theoretically and refined using a riding model. Hydrogens of water were not treated. The crystal data and refinement parameters of **1**–**3** are summarized in table 1. Selected bond lengths and angles of **1**–**3** are listed in table S1.

3. Results and discussions

3.1. *Crystal structure of 1, 2 and 3*

XRD analysis reveals that the structures of **1**–**3** contain the similar Keggin $[PMo_{12}O_{40}]^{3-}$ cluster, which is composed of a central PO_4 tetrahedron surrounded by four vertex-sharing Mo_3O_{13} trimers from association of three edge-sharing MoO_6 octahedra. In **1**, the P–O distances range from 1.530(2) to 1.537(4) Å, O–P–O bond angles are 109.32(10) and 109.62(10)°, respectively. All Mo have a {MoO_6} octahedral environment. Mo–O distances fall into three classes: Mo–Od (terminal) 1.697(3)–1.724(3) Å, Mo–Ob/c (bridge) 1.858(3)–1.975(3) Å, and Mo–Oa (central) 2.411(2)–2.452(2) Å, respectively. The $[PMo_{12}O_{40}]^{3-}$ polyoxoanion is distorted Keggin structure in **2**; the P is located at the inversion center and surrounded by a cube of eight oxygens with each oxygen site half-occupied. The P–O distances range from 1.494(7) to 1.561(7) Å and O–P–O bond angles from 68.9(4) to 179.999(1)°. This structure often appears in $XMo_{12}O_{40}^{n-}$ Keggin structures, explained by several groups [46, 47]. In **3**, the P–O distances range from

1.525(5) to 1.545(3) Å, O–P(1)–O bond angles are 109.46(12) and 109.49(11)°, respectively; O–P(2)–O bond angles are 109.75(11), 109.20(11), and 109.19(12)°, respectively. Molybdenum has a $\{MoO_6\}$ octahedral environment with the Mo–O distances falling into three classes: Mo–Od (terminal) 1.669(3)–1.683(3) Å, Mo–Ob/c (bridge) 1.828(3)–1.994(3) Å, and Mo–Oa (central) 2.422(3)–2.446(3) Å, respectively. According to bond valence sum calculation [48], all Mo have oxidation state +VI (average Calcd value = 5.99), consistent with the overall charge balance of these compounds.

Compound **1** is constructed from three Cu^{II} ions, two Keggin-type $[PMo_{12}O_{40}]^{3-}$ polyanions, six bei ligands, and six lattice waters. Each Cu^{II} joins two bei ligands via Cu–N bonds to form a waved short chain ($Cu(bei)_2^{2+}$). Each $[PMo_{12}O_{40}]^{3-}$ polyanion join three waved short chains to form a wind-wheel shaped structure. $[PMo_{12}O_{40}]^{3-}$ as the wheel hub is located in the center, three waved $Cu(bei)_2^{2+}$ short chains as the vanes are around it in the same direction. Two adjacent $[PMo_{12}O_{40}]^{3-}$ polyanions share a $Cu(bei)_2^{2+}$ short chain to form an infinite 2-D netty structure (figure 1). 2-D layers are further extended to form the 3-D structure via supramolecular interactions. Seen along the crystallographic *c* axis, the whole structure is a honeycomb composed of countless corner-sharing and edge-sharing hexagonal metal–organic ligand units with $[PMo_{12}O_{40}]^{3-}$ polyanions in the cavities of the hexagonal honeycomb (figure 2).

Compound **2** is composed of one Keggin-type $[PMo_{12}O_{40}]^{3-}$, two bbi and two lattice waters, one bbi is mono-protonated, the other is di-protonated. $[PMo_{12}O_{40}]^{3-}$ polyanions are arranged in a line. Bbi are arranged end to end to form an infinite chain; another chain

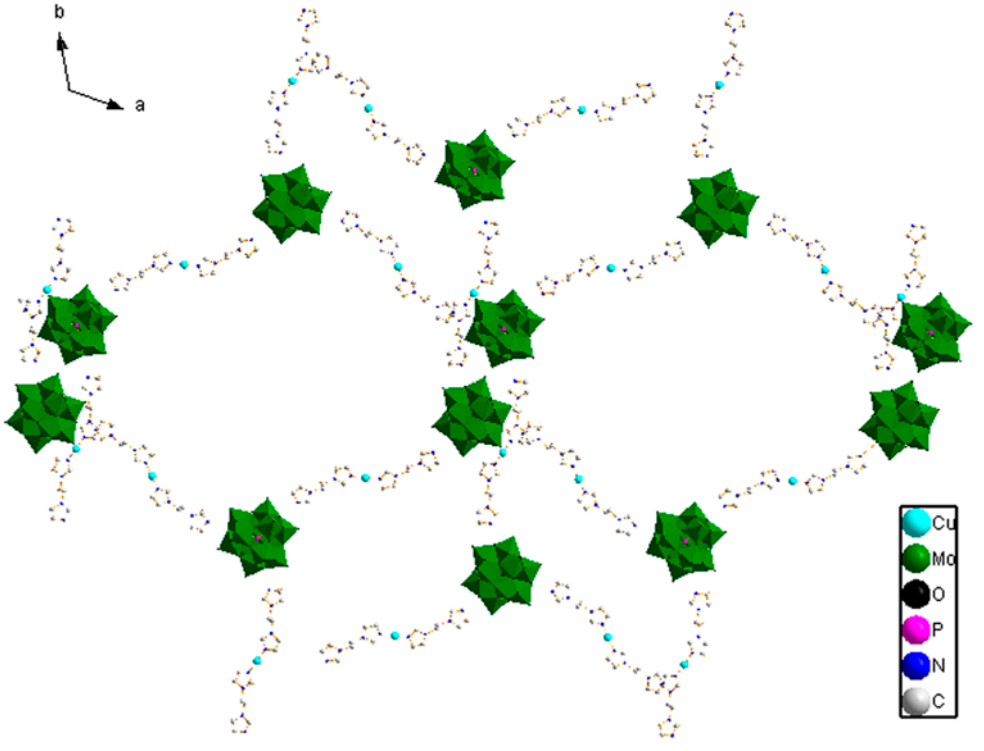

Figure 1. The 2-D supramolecular structure of **1**. All hydrogens were omitted for clarity.

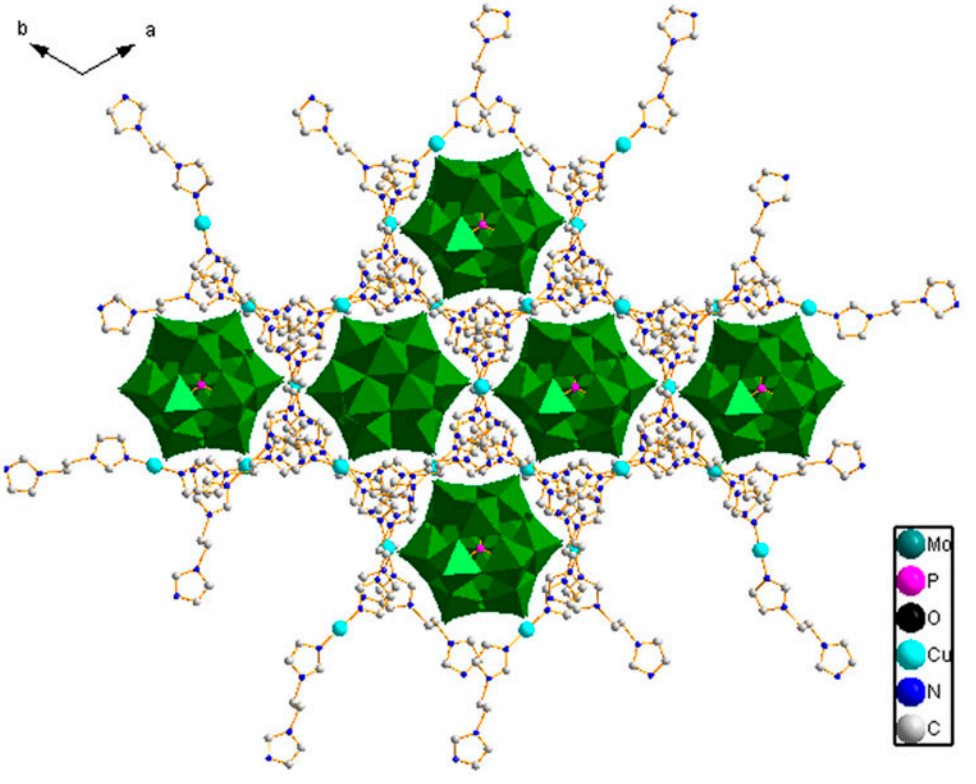

Figure 2. The 3-D supramolecular structure of **1**. All hydrogens were omitted for clarity.

is parallel and misplaced to it. In this way, a double-chain structure is made up. Two such double-chains are located on either side of $[PMo_{12}O_{40}]^{3-}$ polyanions to form a 1-D chain structure (figure 3). Adjacent chains form 2-D layers through sharing of the same double-chains (figure 4). 2-D layers are further extended to form a 3-D structure via supramolecular interactions (figure 5). Water molecules are regularly distributed in the interspace between $[PMo_{12}O_{40}]^{3-}$ chains to stabilize the structure.

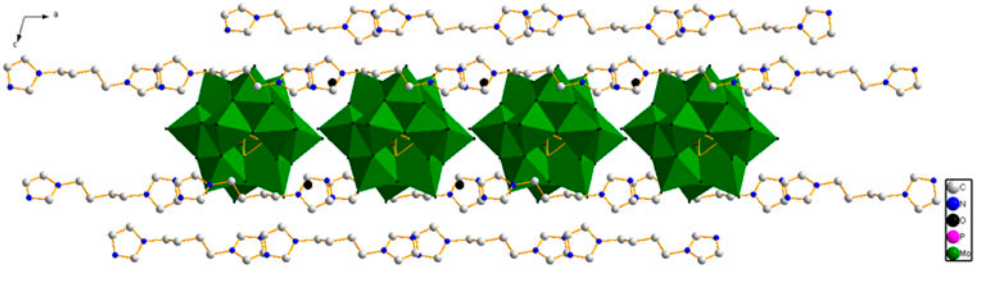

Figure 3. The 1-D structure of **2**. All hydrogens were omitted for clarity.

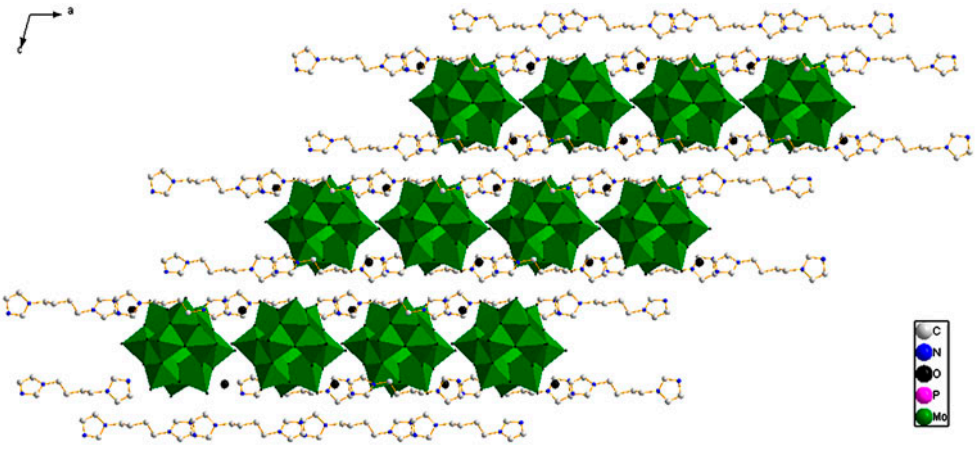

Figure 4. The 2-D structure of **2**. All hydrogens were omitted for clarity.

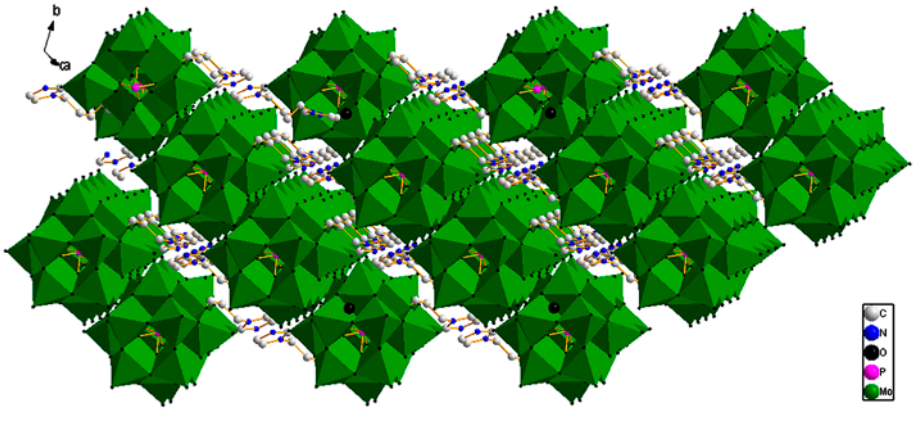

Figure 5. The 3-D structure of **2**. All hydrogens were omitted for clarity.

Compound **3** consists of two Keggin-type $[PMo_{12}O_{40}]^{3-}$, three di-protonated bpp, and six lattice waters. A terminal O(8) and a bridge O(10) of each Keggin cluster centered on the $\{P(2)O_4\}$ tetrahedron are connected with O(2W) and O(1W), respectively, while the two waters are connected with N(1) and N(2) of bpp, respectively. Each bpp is linked with adjacent Keggin clusters through two waters to form an infinite chain (figure 6). The typical hydrogen bonds are as follows: O(1W)…N(2) 2.716(6) Å; O(2W)…N(1) 2.696(6) Å; O(1W)…O(10) 2.867 Å; O(2W)…O(8) 2.932 Å. Each Keggin cluster is also linked with another independent Keggin cluster via supramolecular interactions (O(10)…O(23) 3.023 Å; O(26)…O(23) 3.000 Å). Each independent Keggin cluster of the 1-D chain is connected with crystallographically different Keggin cluster of the third chain via hydrogen bonds between O(8) and O(2W), O(2W) and bpp, bpp and O(1W), and O(1W) and O(10), where O(8) and O(10) belong to two crystallographically different Keggin clusters. This leads to a 2-D layer shown in figure 7. These two-dimensional layers are further extended to a 3-D supramolecular network via hydrogen bonds between O(2W) and N(1), and O(2W) and O(8) (figure 8).

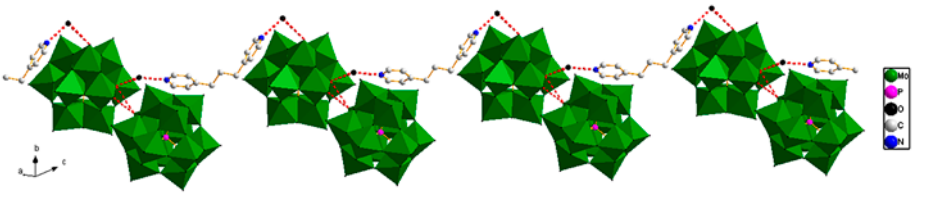

Figure 6. The 1-D chain structure of **3**. All hydrogens were omitted for clarity. The hydrogen bonds are shown by red dotted lines (see http://dx.doi.org/10.1080/00958972.2013.844801 for color version).

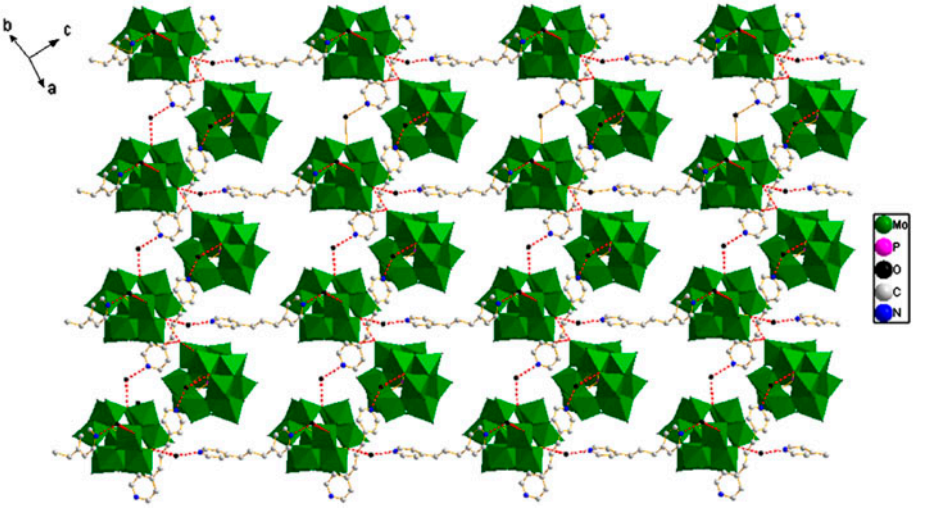

Figure 7. The 2-D layer structure of **3**. All hydrogens were omitted for clarity. The hydrogen bonds are shown by red dotted lines (see http://dx.doi.org/10.1080/00958972.2013.844801 for color version).

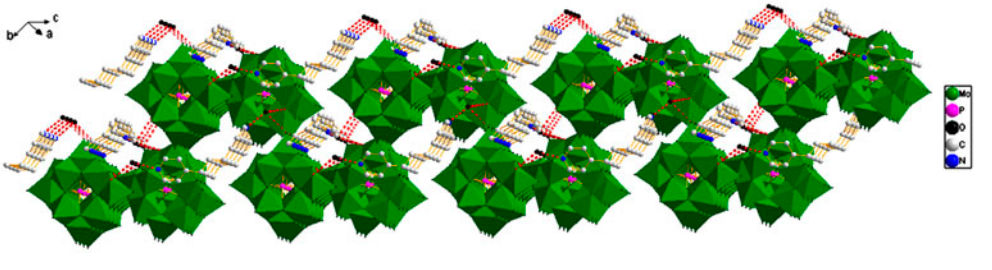

Figure 8. The 3-D network of **3**. All hydrogens were omitted for clarity. The hydrogen bonds are shown by red dotted lines (see http://dx.doi.org/10.1080/00958972.2013.844801 for color version).

3.2. *IR spectrum and XRD*

The IR spectra of **1**–**3** are shown in figure S1. All exhibit the typical bands of Keggin anions from 700 to 1100 cm^{-1}; characteristic bands at 952, 872, 798, and 1057 cm^{-1}

for **1**; 952, 873, 798, and 1057 cm^{-1} for **2**; 967, 886, 787, and 1069 cm^{-1} for **3** correspond to ν(Mo–Od), ν(Mo–Ob–Mo), ν(Mo–Oc–Mo), and ν(P–O) [49]. Bands at 3126, 1623–1234 cm^{-1} for **1**; 2851–3449, 2367, 1623–1163 cm^{-1} for **2**; and 3444, 3141–1070 cm^{-1} for **3** can be assigned to vibrations of water and the ligands [50].

To confirm the purity of **1**–**3**, powder XRD has been performed. The powder XRD patterns of bulk products of **1**–**3** are in agreement with the calculated pattern based on the result from single-crystal XRD, which indicates bulk products for **1**–**3** are pure (figure S2). The difference in intensity may be due to the preferred orientation of the powder sample.

3.3. *TG analysis*

Thermal stabilities of **1**–**3** were determined under nitrogen by TGA (see figure S3) from 25 to 900 °C. For **1**, TGA curve displays two weight losses. The initial weight loss (2.19%) from 117 to 145 °C is attributed to removal of lattice water (Calcd: 2.23%). The second weight loss (19.98%) from 250 to 510 °C corresponds to bei (Calcd: 20.01%). For **2**, TGA curve displays two weight losses. The initial weight loss (1.58%) from 94 to 148 °C is attributed to removal of lattice water (Calcd: 1.61%). The second weight loss (17.04%) from 220 to 476 °C corresponds to bbi (Calcd: 17.00%). For **3**, TGA curve also displays two weight losses. The initial weight loss (2.52%) from 150 to 200 °C is attributed to removal of six lattice waters (Calcd: 2.48%). The second weight loss (13.71%) from 300 to 450 °C corresponds to three bpp (Calcd: 13.73%). The result further confirms the formulas of **1**–**3**.

3.4. *Fluorescent properties*

Luminescent compounds are of interest for various potential applications [51]. Fluorescence spectra of **1**–**3** in the solid state at room temperature were determined (figure 9). Intense emissions occur at ca. 406 nm (λ_{ex} = 347 nm) for **1**, 453 nm (λ_{ex} = 396 nm) for **2**, and 486 and 503 nm (λ_{ex} = 370 nm) for **3**. Emission peaks of **1**–**3** are close to the emission bands of free bei (410 nm) [52], bbi (438 nm) [53], and bpp (446 nm) [54]. Emission maxima of **1**–**3** have blue or red shifts. It is possible that a combination of several factors [55], including a change in the highest occupied molecular orbital and lowest unoccupied molecular orbital energy levels of deprotonated bbi and bei ligands and the intraligand emission from the protonated ligands, contribute to the changes. The results indicate that **1**–**3** are efficient fluorescent materials.

3.5. *Voltammetric behavior*

Owing to the insolubility of **1**–**3** in water, CPE becomes an optimal choice to study the electrochemical properties. The electrochemical behaviors of **1**- to **3**-CPEs have been studied. The cyclic voltammograms in 1 M H_2SO_4 aqueous solution at different scan rates are presented in figure S4. Three reversible redox peaks appear in the potential range −0.8 to 1.0 V. The half-wave potentials $E_{1/2}=(E_{pa} + E_{pc})/2$ (scan rate: 20 mV s^{-1}) are 0.4905 (I–I′), 0.0429 (II–II′), and −0.2472 (III–III′) V for **1**-CPE; 0.4866 (I–I′), 0.0577 (II–II′), and −0.2455 (III–III′) V for **2**-CPE; and 0.4986 (I–I′), 0.0243 (II–II′), and −0.2758 (III–III′) V

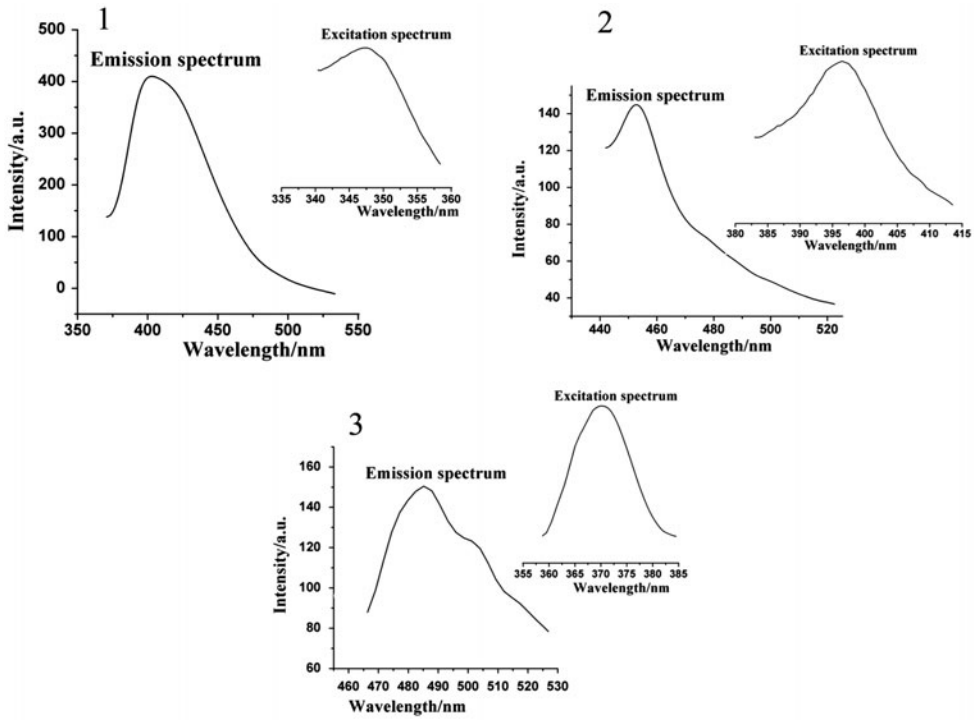

Figure 9. Fluorescence spectra of **1**–**3**.

for **3**-CPE, in accord with three consecutive two-electron processes of Mo(VI/V) couples from PMo_{12} [56, 57]. However, the expected oxidation peak of copper for **1**-CPE is not observed, perhaps due to overlap with the Mo^{VI}/Mo^{V} redox peak, frequently observed in similar PMo/Cu systems [58]. Peak potentials vary gradually following the scan rates from 20 to 160 mV s^{-1} with the cathodic peak potentials shifting toward the negative direction and the corresponding anodic peak potentials to the positive direction with increasing scan rates.

3.6. *Electrocatalysis*

Keggin POMs can be used as electrocatalysts for reduction in nitrite and hydrogen peroxide in aqueous solutions [59, 60]. Figure 10 exhibits cyclic voltammograms for the electrocatalytic reduction in H_2O_2 at **1**- to **3**-CPEs in 1 M H_2SO_4 aqueous solution from −0.8 to 1.0 V. The **1**- to **3**-CPEs display good electrocatalytic activity toward reduction in H_2O_2. With increasing H_2O_2 concentration, all three reduction peak currents gradually increase while the corresponding oxidation peak currents markedly decrease, demonstrating that H_2O_2 is reduced by two-, four-, and six-electron reduced species of PMo_{12} anions [61]. Catalytic activities were improved with increasing extent of POM anion reduction. In contrast, the reduction in H_2O_2 at a bare electrode generally requires a large overpotential, and no obvious response was observed at a bare CPE.

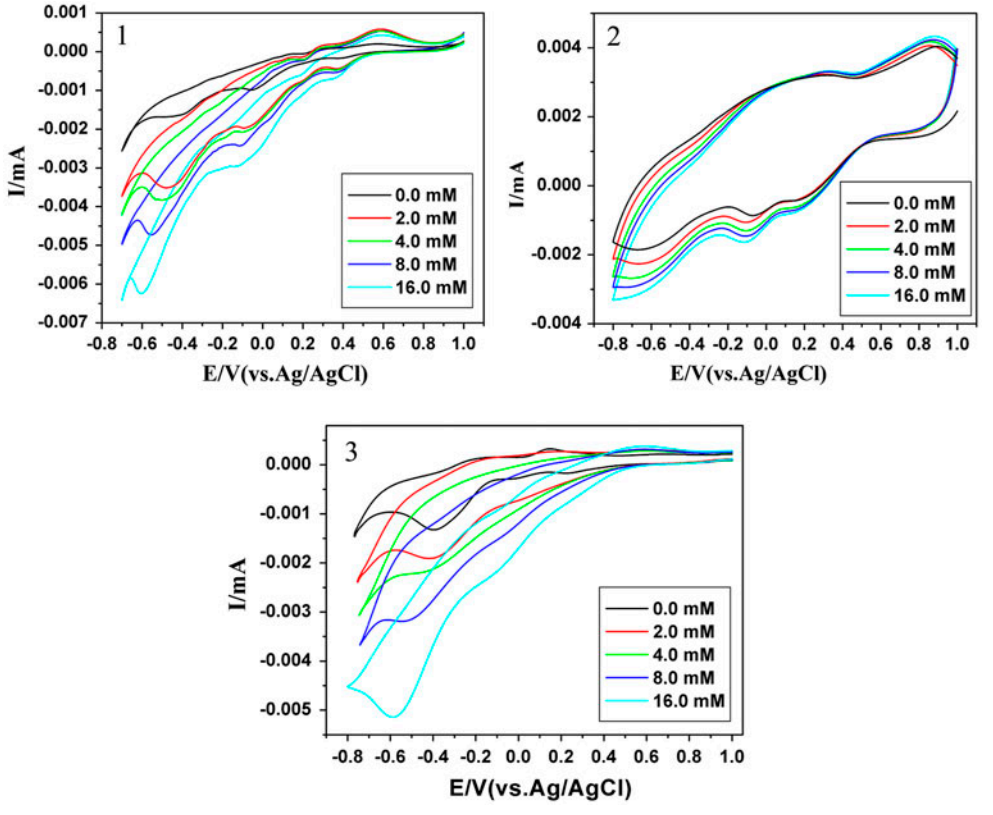

Figure 10. Cyclic voltammograms of the **1**-, **2**- and **3**-CPEs in 1 M H_2SO_4 solution containing 0.0, 2.0, 4.0, 8.0 and 16.0 mM H_2O_2; scan rate: 20 mV s^{-1}.

4. Conclusions

We have prepared and structurally characterized three new supramolecular compounds based on Keggin phosphomolybdate and $[Cu(bei)_2]^{2+}$ complex cations or protonated bbi or bpp cations. In **1**–**3**, Keggin-type POM ($[PMo_{12}O_{40}]^{3-}$) joins to organocations via hydrogen bonding interactions to form various 3-D supramolecular frameworks. This work provides examples of hydrogen bonding interaction in guiding self-assembly of high-dimensional POM-based inorganic metal–organic/organic hybrid supramolecular complexes, opening a pathway for design and synthesis of multifunctional hybrid materials based on POMs and flexible ligands. Further studies are being conducted in our laboratory. Fluorescence exhibits that **1**–**3** are potential fluorescent materials. Electrochemical analysis shows that **1**-, **2**-, and **3**-CPEs display redox properties and good electrocatalytic activity to H_2O_2.

Supplementary material

CCDC 856073, 921874, 678823 contain the supplementary crystallographic data of **1**, **2** and **3**, respectively. These data can be obtained free of charge from The Cambridge

Crystallographic Data Center via www.ccdc.cam.ac.uk/data_request/cif. Related figures and tables, IR spectra, XRD spectra, TG curves and the electrochemical properties for **1–3** can be found in supplementary material. Supplemental data for this article can be accessed http://dx.doi.10.1080/00958972.2013.844801.

Funding

This work is supported by the National Natural Science Foundation of China [grant numbers 20971032, 51172057, and 21271056]; Technological innovation team building program of college of Heilongjiang Province [2009td04]; Innovation Team Research Program of Harbin Normal University [KJTD200902]; The Scientific Innovation Project for Graduate of Heilongjiang Province [number YJSCX2012-188HLJ]; Key Laboratory of Functional Inorganic Material Chemistry (Heilongjiang University), and Ministry of Education and Specialized Research Fund for the Doctoral Program of Higher Education [20122329110001].

References

[1] R. Chakrabarty, P.S. Mukherjee, P.J. Stang. *Chem. Rev.*, **111**, 6810 (2011).
[2] G.S. Kottas, L.I. Clarke, D. Horinek, J. Michl. *Chem. Rev.*, **105**, 1281 (2005).
[3] R.J. Sarma, J.B. Baruah. *Cryst. Growth Des.*, **7**, 989 (2007).
[4] Y.F. Zeng, X. Hu, F.C. Liu, X.H. Bu. *Chem. Soc. Rev.*, **38**, 469 (2009).
[5] M. Du, Y.M. Guo, S.T. Chen, X.H. Bu, S.R. Batten, J. Ribas, S. Kitagawa. *Inorg. Chem.*, **43**, 1287 (2004).
[6] J.R. Li, Y. Tao, Q. Yu, X.H. Bu, H. Sakamoto, S. Kitagawa. *Chem. Eur. J.*, **14**, 2771 (2008).
[7] D. Bradshaw, J.B. Claridge, E.J. Cussen, T.J. Prior, M.J. Rosseinsky. *Acc. Chem. Res.*, **38**, 273 (2005).
[8] F. Xiao, J. Hao, J. Zhang, C. Lv, P. Yin, L. Wang, Y. Wei. *J. Am. Chem. Soc.*, **132**, 5956 (2010).
[9] D.L. Long, R. Tsunashima, L. Cronin. *Angew. Chem. Int. Ed.*, **49**, 1736 (2010).
[10] A. Dolbecq, E. Dumas, C.R. Mayer, P. Mialane. *Chem. Rev.*, **110**, 6009 (2010).
[11] C.L. Hill, J.W. Han. *J. Am. Chem. Soc.*, **129**, 15094 (2007).
[12] Y. Ishii, Y. Takenaka, K. Konishi. *Angew. Chem., Int. Ed. Engl.*, **43**, 2004 (2702).
[13] J.M. Knaust, C. Inman, S.W. Keller. *Chem. Commun.*, 492 (2004).
[14] K. Fukaya, T. Yamase. *Angew. Chem. Int. Ed.*, **42**, 654 (2003).
[15] C.L. Hill. *Chem. Rev.*, **98**, 1 (1998).
[16] C.D. Wu, C.Z. Lu, H.H. Zhuang, J.S. Huang. *J. Am. Chem. Soc.*, **124**, 3836 (2002).
[17] P.J. Hagrman, D. Hagrman, J. Zubieta. *Angew. Chem. Int. Ed.*, **38**, 2638 (1999).
[18] M.T. Pope, A. Müller. *Angew. Chem. Int. Ed. Engl.*, **30**, 34 (1991).
[19] J. Thiel, C. Ritchie, C. Streb, D.L. Long, L. Cronin. *J. Am. Chem. Soc.*, **131**, 4180 (2009).
[20] H.Q. Tan, Y.G. Li, Z.M. Zhang, C. Qin, X.L. Wang, E.B. Wang, Z.M. Su. *J. Am. Chem. Soc.*, **129**, 10066 (2007).
[21] E. Burkholder, J. Zubieta. *Chem. Commun.*, 2056 (2001).
[22] J. Yang, K.L. Huang, Z.F. Pu, Y. Gong, H. Li, C.W. Hu. *J. Mol. Struct.*, **789**, 162 (2006).
[23] P.P. Zhang, J. Peng, J.Q. Sha, A.X. Tian, H.J. Pang, Y. Chen, M. Zhu. *CrystEngComm*, **11**, 902 (2009).
[24] J.Q. Sha, H.Y. Liu, J. Peng, C. Wang, Y.G. Lv, P.P. Zhang. *Z. Naturforsch.*, **65b**, 1 (2010).
[25] K. Yu, B.B. Zhou, Y. Yu, Z.H. Su, C.M. Wang, C.X. Wang. *Inorg. Chem. Commun.*, **14**, 1846 (2011).
[26] L.L. Wen, Z.D. Lu, J.G. Lin, Z.F. Tian, H.Z. Zhu, Q.J. Meng. *Cryst. Growth Des.*, **7**, 93 (2007).
[27] Y.Y. Liu, J.F. Ma, J. Yang, Z.M. Su. *Inorg. Chem.*, **46**, 3027 (2007).
[28] X.-L. Wang, J. Li, A.-X. Tian, D. Zhao, G.-C. Liu, H.-Y. Lin. *Cryst. Growth Des.*, **11**, 3456 (2011).
[29] C.-M. Liu, J.-Y. Zhang, D.-Q. Zhang. *J. Coord. Chem.*, **61**, 627 (2008).
[30] J.Q. Sha, J. Peng, H.S. Liu, J. Chen, A.X. Tian, B.X. Dong, P.P. Zhang. *J. Coord. Chem.*, **61**, 1221 (2008).
[31] J.Y. Guo, X.F. Jin, L. Chen, Z.X. Wang, Y. Xu. *J. Coord. Chem.*, **65**, 3821 (2012).
[32] Y.-B. Liu, Y. Wang, L.-N. Xiao, Y.-Y. Hu, L.-M. Wang, X.-B. Cui, J.-Q. Xu. *J. Coord. Chem.*, **65**, 4342 (2012).
[33] X.-L. Wang, Q. Gao, A.-X. Tian, D. Zhao, X.-J. Liu. *J. Coord. Chem.*, **66**, 358 (2013).
[34] P.P. Zhang, J. Peng, H.J. Pang, Y. Chen, M. Zhu, D.D. Wang, M.G. Liu, Y.H. Wang. *Solid State Sci.*, **12**, 1585 (2010).
[35] H.J. Pang, J. Peng, J.Q. Sha, A.X. Tian, P.P. Zhang, Y. Chen, M. Zhu. *J. Mol. Struct.*, **922**, 88 (2009).

[36] Y.Q. Lan, S.L. Li, X.L. Wang, K.Z. Shao, Z.M. Su, E.B. Wang. *Inorg. Chem.*, **47**, 529 (2008).
[37] K. Jiang, L.F. Ma, X.Y. Sun, L.Y. Wang. *CrystEngComm*, **13**, 330 (2011).
[38] J.S. Qin, D.Y. Du, S.L. Li, Y.Q. Lan, K.Z. Shao, Z.M. Su. *CrystEngComm*, **13**, 779 (2011).
[39] S.Q. Zang, M.M. Dong, Y.J. Fan, H.W. Hou, C.W. Thomas Mak. *Cryst. Growth Des.*, **12**, 1239 (2012).
[40] M.L. Qi, K. Yu, Z.H. Su, C.X. Wang, C.M. Wang, B.B. Zhou, C.C. Zhu. *Inorg. Chem. Commun.*, **30**, 173 (2013).
[41] M.L. Qi, K. Yu, Z.H. Su, C.X. Wang, C.M. Wang, B.B. Zhou, C.C. Zhu. *Inorg. Chim. Acta*, **400**, 59 (2013).
[42] M.L. Qi, K. Yu, Z.H. Su, C.X. Wang, C.M. Wang, B.B. Zhou, C.C. Zhu. *Dalton Trans.*, **42**, 7586 (2013).
[43] C. Rocchiccioli-Deltcheff, M. Fournier, R. Franck, R. Thouvenot. *Inorg. Chem.*, **22**, 207 (1983).
[44] G.M. Sheldrick. *SHELXS-97, Program for X-ray Crystal Structure Refinement*, University of Göttingen, Göttingen, Germany (1997).
[45] G.M. Sheldrick. *SHELXL-97, Program for Crystal Structure Solution*, University of Gőttingen, Germany (1997).
[46] X.L. Wang, Y.F. Bi, B.K. Chen, H.Y. Lin, G.C. Liu. *Inorg. Chem.*, **47**, 2442 (2008).
[47] G.G. Gao, L. Xu, W.J. Wang, X.S. Qu, H. Liu, Y.Y. Yang. *Inorg. Chem.*, **47**, 2325 (2008).
[48] I.D. Brown, D. Altermatt. *Acta Crystallogr., Sect. B: Struct. Sci*, **41**, 244 (1985).
[49] C. Rocchicccioli-Deltcheff, M. Fournier, R. Franck, R. Thouvenot. *Inorg. Chem.*, **2**, 207 (1983).
[50] Y.-Y. Niu, L.-F. Wang, X.-R. Lv, H.-J. Du, Y.-Z. Qiao, H.-M. Wang, L.-S. Song, B.-L. Wu, H.-W. Hou, S.W. Ng. *CrystEngComm*, **13**, 5071 (2011).
[51] T.F. Liu, J. Lü, L.X. Shi, Z.G. Guo, R. Cao. *CrystEngComm*, **11**, 583 (2009).
[52] L.P. Wu, Y. Yamagiwa, T. Kuroda-Sowa, T. Kamikawa, M. Munakata. *Inorg. Chim. Acta*, **256**, 155 (1997).
[53] Y.Y. Liu, J.F. Ma, J. Yang, Z.M. Su. *Inorg. Chem.*, **46**, 3027 (2007).
[54] W.H. Zhang, Z. Dong, Y.Y. Wang, L. Hou, J.C. Jin, W.H. Huang, Q.Z. Shi. *Dalton Trans.*, **40**, 2509 (2011).
[55] S.L. Li, Y.Q. Lan, J.F. Ma, J. Yang, G.H. Wei, L.P. Zhang, Z.M. Su. *Cryst. Growth Des.*, **8**, 675 (2008).
[56] P. Wang, Y. Yuan, Z.B. Han, G.Y. Zhu. *J. Mater. Chem.*, **11**, 549 (2001).
[57] X.L. Wang, H.Y. Lin, Y.F. Bi, B.K. Chen, G.C. Liu. *J. Solid State Chem.*, **181**, 556 (2008).
[58] X.L. Wang, Y.F. Bi, K.B. Chen, H.Y. Lin, G.C. Liu. *Inorg. Chem.*, **47**, 2442 (2008).
[59] B. Keita, A. Belhouari, L. Nadjo, R. Contan. *J. Electroanal. Chem.*, **381**, 243 (1995).
[60] J.E. Toth, F.C. Anson. *J. Electroanal. Chem.*, **361**, 256 (1988).
[61] P. Wang, X.P. Wang, X.Y. Jing, G.Y. Zhu. *Anal. Chim. Acta*, **51**, 424 (2000).